Proceedings of the 7th World Congress on Civil, Structural, and Environmental Engineering (CSEE'22)
~~Lisbon, Portugal~~ Virtual Conference – April 10 – 12, 2022
Paper No. ICSECT 132
DOI: 10.11159/icsect22.132

Shear Strength of Steel Fiber-Reinforced Recycled Aggregates Concrete Deep Beams

Nancy Kachouh, Tamer El-Maaddawy, Hilal El-Hassan, Bilal El-Ariss
United Arab Emirates University
Al Ain, United Arab Emirates
nancy.kachouh@uaeu.ac.ae; tamer.maaddawy@uaeu.ac.ae; helhassan@uaeu.ac.ae; bilal.elariss@uaeu.ac.ae

Abstract **–** The effectiveness of steel fibers to improve the shear behavior of recycled aggregates concrete deep beams is investigated experimentally in this paper. Three large-scale concrete deep beams with a shear span-to-depth ratio (*a/h*) of 1.6 were tested. Two beams had a 100% recycled concrete aggregates (RCA) replacement ratio whereas one beam was made with natural aggregates (NA) to act as a benchmark. One of the RCA beams included steel fibers at a volume fraction of 1%. The use of a 100% RCA significantly impaired the beam stiffness, reduced the cracking load by 25%, and decreased the shear strength by 5%. The use of steel fibers in a RCA beam delayed initiation of shear cracks, improved the beam stiffness, and fully restored the original shear capacity.

Keywords**:** shear, deep beams, steel fibers, recycled concrete aggregates.

1. Introduction

The reuse of aggregates obtained from construction and demolition waste in the building industry is considered a sustainable practice that promises to preserve natural resources and reduce environmental pollution associated with landfills. Despite its promising environmental, ecological, and economic advantages, the use of RCA has been limited to non-structural applications such as road subbases due to a deterioration in their mechanical and durability properties [1-4]. This shift towards sustainable construction and circular economy encouraged researchers to investigate different methods to improve the performance of recycled aggregates concrete [5-8]. For instance, the inclusion of steel fibers in concrete mixtures improved the tensile properties of concrete made with RCA [9]. Such an improvement in tensile properties would enhance the shear response of recycled aggregates concrete beams.

In addition to the mechanical properties of concrete and amount of longitudinal and transverse steel reinforcing bars, the shear strength of recycled aggregates concrete beams was also affected by the RCA replacement percentage, shear span-to-effective depth ratio (*a/d*), and steel fiber volume fraction [10-16]. Concrete beams having 100% RCA and *a/d* of 3 exhibited a shear strength reduction of approximately 10% relative to that of a similar beam with NA [10-11]. In another investigation, it was reported that partial or full replacement of NA with RCA had almost no effect on the shear resistance of concrete beams with *a/d* of 3.5 [12]. Recycled aggregates concrete beams with *a/d* of 1.5 and 3 exhibited shear strength reductions of approximately 10 and 23%, respectively [13]. In turn, the inclusion of steel fibers restricted growth of shear cracks and enhanced the shear response of natural and recycled aggregates concrete beams [14-17].

Beams with $a/h \leq 2$ are considered deep beams [18]. They are typically used as transfer girders in high rise buildings. Limited information is available in the literature on the shear behavior of recycled aggregates concrete deep beams reinforced with steel fibers. This paper reports experimental test results of three large-scale concrete deep beam specimens. Test variables included full replacement of the NA with RCA and the inclusion of steel fibers. Dune sand was used as fine aggregates in all specimens to promote aspects of sustainability. The crack pattern, failure mode, shear strength and deflection response of the RCA deep beam specimens were determined experimentally and compared to those of a benchmark specimen made with NA without fibers.

2. Experimental Program

The present study comprised testing three large-scale concrete deep beams with *a/h* of 1.6. The natural coarse aggregates in two beams were fully replaced by recycled concrete coarse aggregates, whereas one beam was made with natural coarse

aggregates to serve as a benchmark. One of the recycled aggregates concrete deep beams did not include fibers whereas the other one incorporated 1% steel fibers, by volume.

2.1. Materials

The concrete constituent materials included ASTM Type I ordinary Portland cement (OPC), coarse aggregates in the form of RCA and NA, desert dune sand, and tap water. Natural aggregates were crushed dolomitic limestone. Recycled aggregates were obtained from a local concrete recycling plant that used demolition waste of old concrete structures to produce recycled coarse aggregates. Their properties and particle size distribution can be found elsewhere [2]. The RCA and NA were used in a saturated surface dry (SSD) condition to account for their water absorption. The control mix was designed and prepared based on ACI 211.1 [19] to achieve a target cylinder concrete compressive strength (f'_c) of 30 MPa. The concrete mix proportion ratios, by weight, were cement: fine aggregates: coarse aggregates: w/c of 1:1.2:2.4:0.49. Three 150-mm cubes and six cylinders 150 mm x 300 mm (diameter and height) were sampled. The cubes were used to determine the cube compressive strength of the concrete (f_{cu}) in accordance with BS 12390-3 [20]. Three cylinders were used to obtain f'_c as per ASTM C39 [21], while the other three were utilized to determine the splitting tensile strength (f_{sp}) as per ASTM C496 [22]. The average strength values of the mixes are reported in Table 1. The longitudinal steel reinforcing bars had a yielding stress of 540 MPa and a Young's modulus of 200 GPa. The steel fibers used in this study were hooked at both ends with a tensile strength of 1345 MPa, Young's modulus of 21 GPa, mean diameter (d_f) of 0.55 mm, mean length (l_f) of 35 mm, and an aspect ratio (l_f/d_f) of 65.

Table 1: Concrete properties.

Mix Designation	f'_c (MPa)	f_{cu} (MPa)	f_{sp} (MPa)
R0SF0	36.4 ± 1.5	40.5 ± 1.8	3.1 ± 0.2
R100SF0	23.6 ± 0.4	24.7 ± 1.0	2.1 ± 0.2
R100SF1	25.8 ± 0.3	32.2 ± 0.6	3.1 ± 0.1

2.2. Test Specimens

The deep beam specimens were designated using the notation BRX-SFY, where 'X' is the RCA replacement percentage and 'Y' is the steel fibers volume fraction. Specimen BR0-SF0 designates the control beam made of NA without steel fibers. The remaining two specimens were made of RCA-based concrete: one specimen without steel fibers (BR100-SF0) and another one with a 1% steel fibers volume fraction (BR100-SF1). Other than the replacement of NA by RCA and addition of steel fibers, no changes were made to the specimen dimensions or reinforcement. Details of a typical test specimen are shown in Figure 1. The beam specimens were 3300 mm long with an effective span of 2900 mm and cross-section width and depth of 150 and 500 mm, respectively. The concrete cover to the center of the steel reinforcement was 50 mm, rendering an effective depth of d = 450 mm. The beam shear span was 800 mm, which corresponded to a/h of 1.6. The longitudinal tensile and compressive steel reinforcements consisted of 4 No. 25 (25 mm in diameter) and 2 No. 25 steel bars, respectively. Steel plates (150 × 150 × 20 mm) were used at the load and support locations.

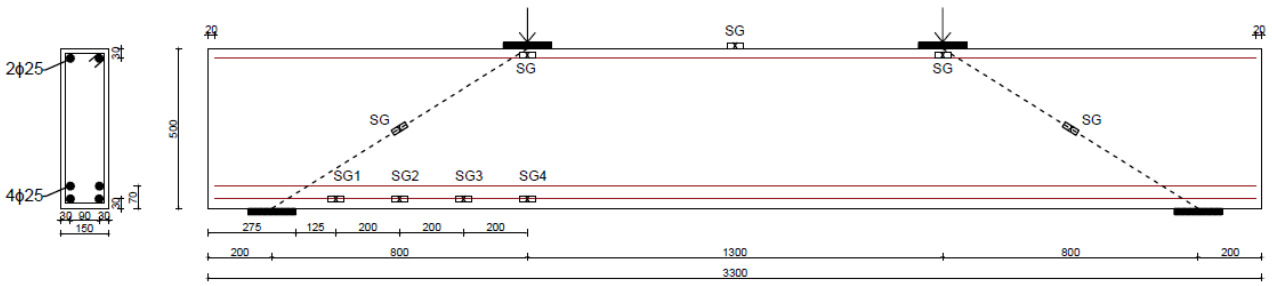

Fig. 1: Details of a typical test specimen (dimension are in mm).

2.3. Test Setup

The concrete deep beams were tested to failure under four-point bending. The load was applied on two points 1300 mm mm apart at the top surface of the beam using two actuators. The tests were initially conducted under a load-control at a rate a rate of 0.5 kN/sec. Prior to reaching the ultimate load, the loading scheme was switched to a displacement control at a rate rate of 0.6 mm/min for safety consideration. The applied loads of the actuators were recorded by two load cells. Linear variable differential transducers (LVDTs) were placed below the beam at mid-span and at the supports to measure the net deflection. The net deflection was calculated as the difference between the measured mid-span deflection and the average of the deflection at the supports. Strain gauges (SG) were bonded to the concrete surface, 60 mm long each, in the longitudinal direction at the midspan and under the loading points and also in the diagonal direction at the middle of each shear span. Also, four strain gauges, 5 mm long each, were attached to the longitudinal steel reinforcing bars within the shear span at a spacing of 200 mm to measure steel strains. The load cells, LVDTs, and strain gauges were connected to a data acquisition system. The front surface of the beams was painted white before testing to monitor the development of cracks during testing.

3. Results and Discussions

The results obtained from laboratory testing of concrete deep beams are presented and discussed. The overall behavior of the deep beam specimens was evaluated based on the load-deflection response, shear resistance, crack pattern, failure mode, and strain measurements. The effectiveness of adding steel fibers to improve the shear response was elucidated.

3.1. Load-Deflection Response

The load-deflection responses of the tested beams are presented in Figure 2. The ascending part of the deflection response of specimens BR0-SF0 and BR100-SF0 consisted of two linear segments with the first being steeper than the second. Initiation of the first shear crack changed the slope of the load-deflection response. After cracking, the deflection increased at a higher rate. The pre-cracking and post-cracking stiffnesses of BR100-SF0 were significantly lower than those of BR0-SF0. Specimen BR0-SF0 reached its shear capacity at a midspan deflection of 7.2 mm whereas specimen BR100-SF0 showed a higher deflection of 9.0 mm at ultimate load. The use of steel fibers with a volume fraction of 1% improved the response of BR100-SF1. The pre-cracking stiffness of BR100-SF1 almost coincided with that of BR100-SF0. Yet, the first visible shear crack did not result in a noticeable change in the slope of the load-deflection response of BR100-SF1. Specimen BR100-SF1 reached its shear capacity at a deflection of 8.2 mm.

The main test results are summarized in Table 2. The NA-based control specimen BR0-SF0 exhibited the first visible shear crack at a load value of V_{cr} = 120 kN, whereas its shear capacity (V_{max}) was 203 kN (i.e. V_{cr}/V_{max} = 0.6). Conversely, the shear cracking load of specimen BR100-SF0 (90 kN) was 25% lower than that of BR0-SF0. However, its shear capacity (193 kN) was only 5% lower. In turn, the replacement of NA by a 100% RCA reduced V_{cr}/V_{max} to a value of approximately 0.5. The addition of 1% steel fibers, by volume, delayed the initiation of shear cracks and improved the shear resistance of BR100-SF1. The value of V_{cr}/V_{max} for specimen BR100-SF1 was approximately 0.7 and its shear capacity was 16 and 22% higher than those of BR100-SF0 and BR0-SF0, respectively. Steel strains in all beams were less than the yield strain as planned in the design. The beams reached their shear capacity at maximum longitudinal concrete strain values in the range of 1400 to 2125 $\mu\varepsilon$ and diagonal concrete strain values of 400 to 1150 $\mu\varepsilon$. Specimen BR100-SF1 exhibited the highest diagonal concrete strain at shear capacity. It seems that the presence of steel fibers allowed the beam to sustain higher diagonal strains prior to failure.

Table 2: Summary of test results.

Specimen	Shear Cracking Stage		Ultimate Stage		Steel Strain[1] ($\mu\varepsilon$)	Concrete Strain[1] ($\mu\varepsilon$)	
	V_{cr} (kN)	Δ_{cr} (mm)	V_{max} (kN)	Δ_{max} (mm)[1]		Longitudinal strain	Diagonal strain
BR0-SF0	120	2.6	203	7.2	1286	2125	400
BR100-SF0	90	2.9	193	9.0	2452	1400	730
BR100-SF1	160	4.6	235	8.2	1689	1650	1150

[1]At ultimate load

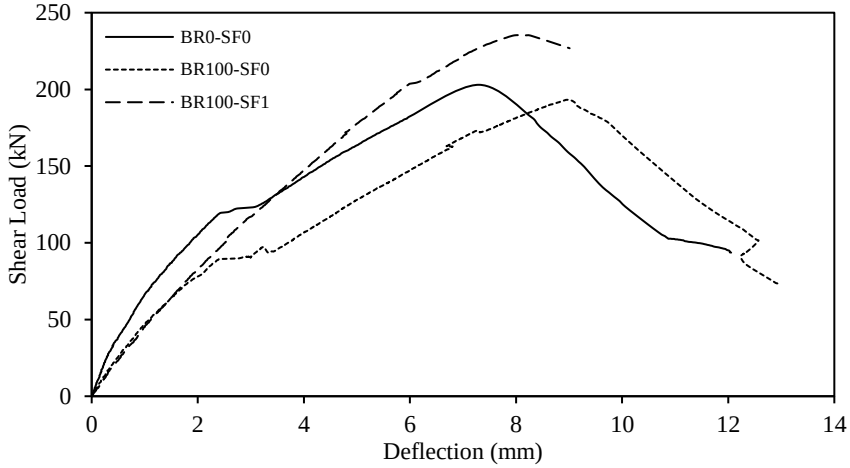

Fig. 2: Shear load-deflection response.

3.2. Crack Pattern and Failure Mode

Schematic drawings of the crack pattern and photographs of the beams at failure are shown in Figure 3. All beams failed in shear. The first shear crack initiated at mid-height of the beam in the shear span then propagated towards the load and support points as the load progressed. Specimens BR0-SF0 and BR100-SF0 exhibited also splitting cracks parallel to the longitudinal steel reinforcing bars in parts of the shear span closer to the support point. A diagonal splitting crack was developed at the onset of failure of specimen BR0-SF0 accompanied by crushing of concrete at the top part of the diagonal concrete strut. Specimen BR100-SF0 exhibited additional shear cracks in the west shear span prior to failure. Specimen BR100-SF0 eventually failed due to local crushing of the concrete above the head of the major diagonal crack developed in the shear span. Spalling of concrete was also observed at the level of the longitudinal reinforcement at crack intersection points. The presence of steel fibers in specimen BR100-SF1 prevented formation of additional shear cracks in shear span. Specimen BR100-SF1 eventually failed due to excessive widening of the major shear crack developed in the west shear span accompanied by local crushing of concrete at the top and bottom parts of the diagonal strut.

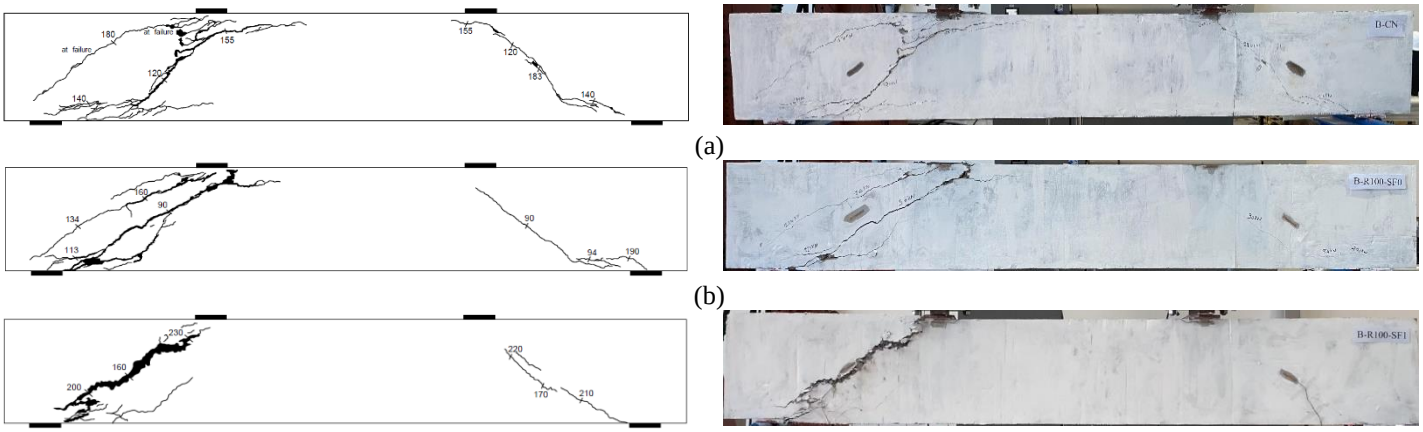

Fig. 3: Crack pattern at failure; (a) BR0-SF0, (b) BR100-SF0, (c) BR100-SF1

3.3. Steel Strain Profile

Figure 4 presents the steel strain profile within the shear span at four different loading stages: 25%, 50%, 75%, and 100% of the shear strength. Specimens BR0-SF0 and BR100-SF1 exhibited almost a uniform steel strain profile within the shear span at all stages of loading, which confirmed the occurrence of the deep beam action. Specimen BR100-SF0 exhibited an almost uniform strain profile within the shear span until it reached approximately 50% of the shear strength. At higher values of load, local spalling of concrete caused by intersection of cracks at a distance 200 mm from the support resulted in increasing the steel strain at this location to a level higher than those recorded at other locations with the shear span.

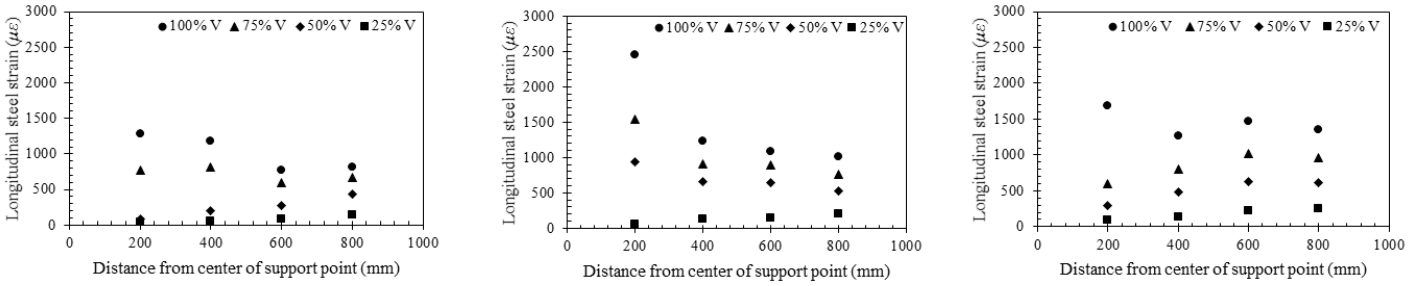

Fig. 4: Steel strain profile; (a) BR0-SF0, (b) BR100-SF0, (c) BR100-SF1

4. Conclusion

Test results of three large-scale concrete deep beam specimens with *a/h* of 1.6 are reported in this paper. One beam was made with NA and two beams were made with RCA. One of the beams with RCA included steel fibers at a volume fraction of 1%. The main conclusions of the work are summarized below.

(i) The use of a 100% RCA in a concrete deep beam resulted in a 25% reduction in the shear cracking load and a 5% reduction in the shear strength compared to those of a NA-based control beam. The recycled aggregates concrete deep beam also exhibited a significant reduction in the stiffness relative to that of the NA-based concrete beam.

(ii) The use of steel fibers with 1% volume fraction in a RCA beam delayed initiation of shear cracks and improved the stiffness. The value of V_{cr}/V_{max} was 0.7 for the RCA beam with steel fibers, but it was in the range of 0.5 to 0.6 for the beams without steel fibers.

(iii) The inclusion of 1% steel fibers, by volume, in a RCA beam fully restored the original shear capacity. The shear strength of the RCA beam with steel fibers was 22% higher than that of the RCA concrete beam without fibers and 16% higher than that of the NA-based concrete beam.

Acknowledgements

The authors would like to acknowledge the financial support provided by UAE University; grant number: 31N372.

References

[1] F. Debieb, L. Courard, S. Kenai and R. Degeimbre, "Mechanical and durability properties of concrete using contaminated recycled aggregates," *Cem Concr Compos*, vol. 32, no. 6, pp. 421-426, 2010.

[2] N. Kachouh, H. EL-Hassan and T. El-Maaddawy, "Effect of steel fibers on the performance of concrete made with recycled concrete aggregates and dune sand," *Constr Build Mater*, vol. 213, pp. 348-359, 2019.

[3] M. Guo, F. Grondin, A. Loukili, "Numerical analysis of the failure of recycled aggregate concrete by considering the random composition of old attached mortar," *J Build Eng*., 28: 101040, 2020.

[4] M. Alzard, H. El-Hassan, and T. El-Maaddawy, "Life Cycle Inventory for the Production of Recycled Concrete Aggregates in the United Arab Emirates", *International Journal of Civil Infrastructure*, vol. 4, 78-84, 2021.

[5] M. Malešev, V. Radonjanin and S. Marinković, "Recycled concrete as aggregate for structural concrete production," *Sustainability*, 2, 1204, 2010.
[6] D. Gao, L. Zhang and M. Nokken, "Compressive behavior of steel fiber reinforced recycled coarse aggregate concrete designed with equivalent cubic compressive strength," *Constr Build Mater*, 141, 235-244, 2017.
[7] N. Kachouh, H. El-Hassan and T. El-Maaddawy, "The Use of Steel Fibers to Enhance the Performance of Concrete made with Recycled Aggregate," *Fifth International Conference on Sustainable Construction Materials and Technologies At: Kingston*, UK, DOI: 10.18552/2019/IDSCMT5012, July 2019.
[8] S. Shoaib, H. El-Hassan, B. El-Ariss, B., and T. El-Maaddawy, "Workability and Early-Age Strength of Recycled Aggregate Concrete Incorporating Basalt Fibers", *International Journal of Civil Infrastructure*, vol. 4, 68-77, 2021.
[9] N. Kachouh, H. El-Hassan and T. El-Maaddawy, "Influence of steel fibers on the flexural performance of concrete incorporating recycled concrete aggregates and dune sand," *J Sust Cem Based Mater*, DOI: 10.1080/21650373.2020.1809546, 2020.
[10] K.N. Rahal and Y.T. Alrefaei, "Shear strength of recycled aggregate concrete beams containing stirrups," *Constr Build Mater*, vol. 191, pp. 866-876, 2018.
[11] F. Al Mahmoud, R. Boissiere, C. Mercier and A. Khelil, "Shear Behavior of Reinforced Concrete Beams Made from Recycled Coarse and Fine Aggregates," *Structures*, 25, 660–669, 2020.
[12] I.S. Ignjatović, S.B. Marinković and N. Tošić, "Shear behaviour of recycled aggregate concrete beams with and without shear reinforcement," *Engineering Structures*, 141, 386-401, 2017.
[13] G. Wardeh and E. Ghorbel, "Shear strength of reinforced concrete beams with recycled aggregates," *Advances in Structural Engineering*, Vol. 22(8) 1938–1951, 2019.
[14] H.H. Dinh, G.J. Parra-Montesinos and J.K. Wight, "Shear behavior of steel fiber-reinforced concrete beams without stirrups reinforcement," *ACI Structural Journal*, vol. 107, no. 5, pp. 597-606, 2010.
[15] A. Amin and S.J. Foster, "Shear strength of steel fibre reinforced concrete beams with stirrups," *Engineering Structures*, 111, 323-332, 2016.
[16] T. Do-Dai, D.T. Tranb and L. Nguyen-Minha, "Effect of fiber amount and stirrup ratio on shear resistance of steel fiber reinforced concrete deep beams", *Journal of Science and Technology in Civil Engineering*,15 (2): 1–13, 2021.
[17] H.R. Chaboki, M. Ghalehnovi, A. Karimipour, J. Brito and M. Khatibinia, "Shear behaviour of concrete beams with recycled aggregate and steel fibres," *Constr Build Mater*. ;204: 809–27, 2019.
[18] ACI 318-14, "Building code requirements for structural concrete and commentary", American Concrete Institute (ACI), Farmington Hills, MI, 2014.
[19] ACI 211.1, "Standard practice for selecting proportions for normal, heavyweight, and mass concrete", Farmington Hills, Michigan.: American Concrete Institute, 2002.
[20] BS EN 12390-3, "Testing hardened concrete - Compressive strength of test specimens", British Standard, London, UK, 2009.
[21] ASTM C39, "Standard Test Method for Compressive Strength of Cylindrical Concrete Specimens", ASTM, West Conshohocken, PA, 2015.
[22] ASTM C496 / C496M-17, "Standard Test Method for Splitting Tensile Strength of Cylindrical Concrete Specimens", ASTM International, West Conshohocken, PA, 2017.